Fundus Image Classification Using Wavelet Based Features in Detection of Glaucoma

D. Selvathi[1], N.B. Prakash[2]*, V. Gomathi[3] and G.R. Hemalakshmi[3]

[1]Department of Electronics and Communication Engineering,
Mepco Schlenk Engineering College, India.
[2]Department of Electrical and Electronics Engineering, [3]Department of Computer Science and
Engineering, National Engineering College, India.
*Corresponding author E-mail: nbprakas@gmail.com

Glaucoma frequently called as the "noiseless hoodlum of sight". The main source of visual impairment worldwide beside Diabetic Retinopathy is Glaucoma. It is discernible by augmented pressure inside the eyeball result in optic disc harm and moderate however beyond any doubt loss of vision. As the renaissance of the worsened optic nerve filaments isn't suitable medicinally, glaucoma regularly goes covered up in its patients anticipating later stages. All around it is assessed that roughly 60.5 million individuals beyond 40 years old experience glaucoma in 2010. This number potentially will lift to 80 million by 2020. Late innovation in medical imaging provides effective quantitative imaging alternatives for the identification and supervision of glaucoma. Glaucoma order can be competently done utilizing surface highlights. The wavelet channels utilized as a part of this paper are daubechies, symlet3 which will expand the precision and execution of classification of glaucomatous pictures. These channels are inspected by utilizing a standard 2-D Discrete Wavelet Transform (DWT) which is utilized to separate features and examine changes. The separated features are sustained into the feed forward neural system classifier that classifies the normal images and abnormal glaucomatous images.

Keywords: Fundus, Glaucoma, frontal chamber.

Glaucoma makes harm the eye's optic nerve and deteriorates after a period of time as shown in Figure. 1. It's frequently connected with a development of pressure inside the eye. The expanded pressure, called intraocular pressure can harm the optic nerve which passes on the pictures to our brain. On the off chance that harms to the optic nerve from high eye pressure proceeds with, glaucoma will cause perpetual loss of vision.

There is a little space in front of eye named as the "frontal chamber". Clear fluid streams all through the foremost chamber which feeds and showers adjacent tissues. On the off chance that a patient has glaucoma, the liquid does not deplete appropriately - it empties too gradually - from the eye. This prompts liquid develop, and weight inside the eye rises. Unless this weight is cut down and controlled, the optic nerve and different parts of the eye may wind up harmed, prompting loss of vision. Without treatment, glaucoma can cause add up to perpetual visual deficiency within a couple of years. Since the vast majority with glaucoma

have no early indications or agony from this expanded pressure, it is critical to see eye specialist frequently so glaucoma can be analyzed and treated after a short time term visual misfortune happens. Glaucoma has a chance to occur over 40 age and family history of glaucoma. It is necessary to have a complete eye exam once in every two year. If left untreated the patient may loss vision, and even become blind. The disease generally affects both eyes, although one may have more severe signs and symptoms than the other.

Literature survey

The most important step in the development process of the automation system is the documentation of comprehensive review of the published and unpublished work from secondary data sources in the areas of specific interest to the researcher. A review more often than not goes before the proposed framework and results segment. Its definitive objective is to convey the reader in the know regarding outgoing flow and structures the reason for another objective. A very much organized survey is described by an intelligent stream of thoughts, momentum and applicable references with predictable, suitable

referencing style, appropriate utilization of wording, and a fair and extensive perspective of the past research on the theme.

Ganesh Babu *et al* present a new method for detection of glaucoma in the retinal images. The proposed system has three stages such as ROI Extraction, Feature Extraction and Classification. Digital image processing methods, for example, preprocessing, morphological tasks and thresholding, are generally utilized for the programmed recognition of optic disc, veins and estimation of the features. The features extracted are Cup to Disc Ratio (CDR) and the proportion of vessel area. K-means clustering method is utilized to compute the CDR feature and are validated by classifying the normal and glaucoma images using neural network classifier.

Acharya *et al* introduced glaucoma detection utilizing a mix of texture and higher order spectra (HOS) features. The results show that the texture and HOS includes after z-score standardization and feature determination, and when joined with a random forest classifier, performs superior to anything alternate classifiers and accurately distinguishes the glaucoma images with a decent exactness. The effect of feature positioning and standardization is additionally
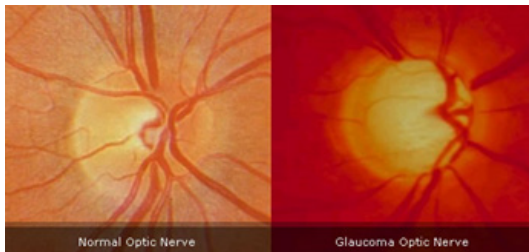

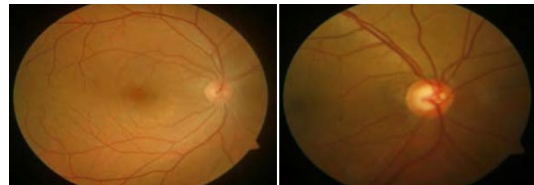**Fig. 1 .** a) Normal Optic Nerve b) Glaucoma Optic Nerve

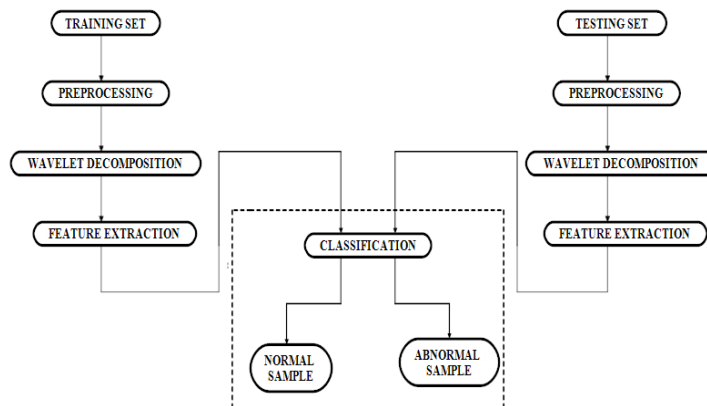**Fig. 2.** Typical fundus images-normal and glaucoma

Fig.3. Proposed Methodology

concentrated to enhance the outcomes. The features are clinically noteworthy and can be utilized to identify glaucoma precisely.

Huang.K *et al* done vitality circulation over wavelet sub groups is a generally utilized element for wavelet packet based texture arrangement. Because of the over total nature of the wavelet packet disintegration; include determination is typically connected for better grouping precision and minimal element portrayal. The larger part of wavelet feature choice calculations lead include choice in light of the assessment of each sub band independently, which verifiably accept that the wavelet features from various sub groups are autonomous. The reliance between features from various sub groups is researched hypothetically

and mimicked for a given picture demonstrates. In view of analysis and simulation, a wavelet feature determination calculation in view of factual reliance is proposed. This algorithm is additionally enhanced by joining the reliance between wavelet include and the assessment of individual wavelet feature part. The results show the viability of the algorithms in fusing reliance into wavelet feature determination.

A.Arivazhagan *et al* defines the use of wavelet transform for classifying the texture of images by describing a new method of feature extraction for description and segmentation of texture at numerous scales based on block by block assessment of wavelet co-occurrence features. The steps involved in feature segmentation are
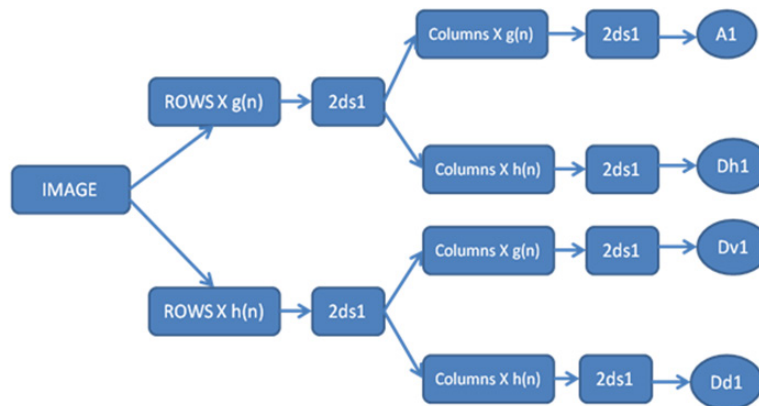

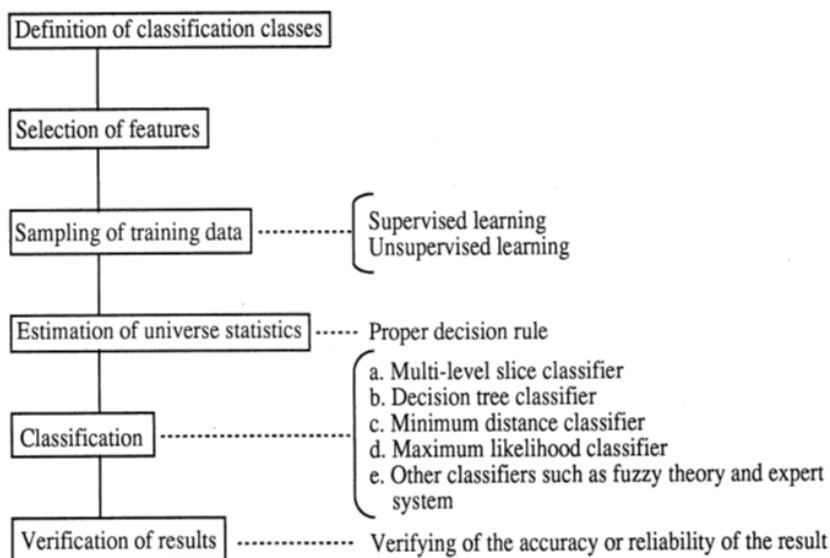**Fig. 4.** 2D DWT Decomposition

Fig. 5. Classification System

decomposition of sub-image block, extraction, and successive block feature difference, and segmentation band, post processing and thinning. The execution of this algorithm is better than conventional single determination strategies, for example, texture spectrum, co-events and so on. The aftereffects of the proposed algorithm are observed to be acceptable. Efficiency is improved by removing noise using disk ûltering and thresholding techniques.

Paul Y. Kim *et al* explores the utilization of fractal examination (FA) as the premise of a framework for multiclass forecast of the movement of glaucoma. FA is connected to pseudo 2-D pictures changed over from 1-D retinal nerve fiber layer information acquired from the eyes of ordinary subjects, and from subjects with dynamic and non dynamic glaucoma. FA features are acquired utilizing a box-counting technique and a multifractional Brownian movement strategy

Table 1. Glaucoma image-horizontal detail

Image	Red	Average Green	Blue	Energy	Standard Deviation	Variance
1_g	0.4812	0.8771	1.0113	7.5687e-007	18.9651	1.0240e+007
2_g	0.4318	0.5440	0.6198	1.3168e-010	0.2510	0.2849
3_g	0.3098	0.5161	0.5870	1.0832e-010	0.2023	0.1428
4_g	0.4033	0.5475	0.6367	1.1462e-010	0.1848	0.1120
5_g	0.4646	0.5552	0.6490	1.3220e-010	0.2374	0.2365
6_g	0.4860	0.4590	0.5319	7.2313e-011	0.1713	0.0675
7_g	0.2435	0.5227	0.6208	1.8193e-010	0.4990	3.4628
8_g	0.3384	0.4717	0.5618	8.5429e-011	0.2072	0.1393
9_g	0.4299	0.5456	0.6596	1.6108e-010	0.3100	0.5052
10_g	0.5223	0.4949	0.5719	9.8881e-011	0.2313	0.1655
11_g	0.5302	0.4909	0.5817	9.0322e-011	0.1785	0.0817
12_g	0.5231	0.5116	0.5937	1.2108e-010	0.2562	0.5398
13_g	0.4512	0.6618	0.7664	2.1839e-007	6.0759	2.4196e+005
14_g	0.4432	0.4504	0.5261	6.0745e-011	0.1477	0.0395
15_g	0.4992	0.4715	0.5540	7.7145e-011	0.1974	0.1634

Table 2. Healthy image-horizontal detail

Image	Red	Average Green	Blue	Energy	Standard Deviation	Variance
1_h	0.6136	0.6112	0.7181	1.6934e-010	0.1974	0.1681
2_h	0.6679	0.7609	0.8839	1.8858e-007	4.2578	9.3808e+004
3_h	0.6645	0.6209	0.7246	1.8141e-010	0.2396	0.3420
4_h	0.6734	0.8035	0.9290	4.0788e-007	6.2043	4.0729e+005
5_h	0.6251	0.6057	0.7140	1.6570e-010	0.2160	0.2110
6_h	0.5842	0.5475	0.6378	1.1106e-010	0.1723	0.0885
7_h	0.4696	0.5197	0.6171	9.1439e-011	0.1533	0.0569
8_h	0.5297	0.5186	0.6055	9.1857e-011	0.1590	0.0594
9_h	0.5945	0.6513	0.7768	1.0330e-007	3.7624	4.7189e+004
10_h	0.2628	0.4721	0.5608	8.1885e-011	0.2025	0.1241
11_h	0.4195	0.4770	0.5638	8.9989e-011	0.2338	0.2123
12_h	0.4485	0.4382	0.5278	5.7557e-011	0.1412	0.0317
13_h	0.4208	0.4196	0.4983	4.7774e-011	0.1477	0.0406
14_h	0.5008	0.4477	0.5305	5.9895e-011	0.1514	0.0437
15_h	0.4271	0.4704	0.5668	7.6932e-011	0.1726	0.0710

that consolidates texture and multiresolution examinations. The two features are utilized for Gaussian kernel based multiclass classification. Sensitivity, specificity, and area under receiver operating characteristic (AUROC) are computed for the FA features and for measurements got utilizing Wavelet-Fourier analysis (WFA) and Fast-Fourier analysis (FFA). Synchronous multiclass characterization among progressors, nonprogressors, and visual typical subjects has not been already portrayed. The novel FA-based features accomplish better execution with less features and less computational than WFA and FFA.

Jun Cheng *et al* proposes optic disc and optic cup segmentation using super pixel classification for glaucoma screening. In optic disc segmentation, histograms, and center surround statistics are used to classify each super pixel as disc or non-disc. For optic cup division, notwithstanding the histograms and focus encompass measurements, the area data is likewise included into the component space to

Table 3. Healthy image vertical detail

Image	Average Red	Green	Blue	Energy	Standard Deviation	Variance
1_h	0.4508	0.4456	0.5132	5.3351e-011	0.2550	0.1157
2_h	0.5461	0.5050	0.5731	9.1708e-011	0.3231	0.4364
3_h	0.4949	0.4594	0.5318	5.9957e-011	0.2590	0.1239
4_h	0.5882	0.7387	0.8566	5.4588e-007	5.3246	1.4883e+005
5_h	0.4624	0.4403	0.5049	4.9679e-011	0.2424	0.0851
6_h	0.4870	0.4583	0.5223	5.8817e-011	0.2603	0.1235
7_h	0.4648	0.5063	0.5808	8.8520e-011	0.3057	0.2697
8_h	0.5113	0.4977	0.5674	7.9265e-011	0.2814	0.2113
9_h	0.5818	0.7459	0.9042	1.4748e-006	9.7181	1.4898e+006
10_h	0.2536	0.4556	0.5393	6.5747e-011	0.3123	0.3574
11_h	0.3747	0.4115	0.4852	4.5316e-011	0.2891	0.3297
12_h	0.4369	0.4296	0.5009	5.2482e-011	0.2868	0.2666
13_h	0.4613	0.4480	0.5412	6.2309e-011	0.3178	0.3830
14_h	0.4756	0.4285	0.5024	5.0414e-011	0.2839	0.2654
15_h	0.4141	0.4519	0.5419	6.8852e-011	0.3400	0.4976

Table 4. Glaucoma image vertical detail

Image	Average Red	Green	Blue	Energy	Standard Deviation	Variance
1_g	0.4310	0.7237	0.8336	1.4816e-007	4.8549	1.2669e+005
2_g	0.4547	0.5645	0.6166	2.3765e-010	0.8150	26.5541
3_g	0.3236	0.5283	0.5964	1.1447e-010	0.3785	0.8233
4_g	0.3800	0.5128	0.5779	9.6839e-011	0.3348	0.4559
5_g	0.4006	0.4552	0.5327	5.5548e-011	0.2474	0.1009
6_g	0.4794	0.4379	0.5222	5.6051e-011	0.2986	0.2805
7_g	0.2419	0.4571	0.5443	6.7806e-011	0.3190	0.3853
8_g	0.3160	0.4332	0.5015	5.3473e-011	0.2918	0.2658
9_g	0.3541	0.4269	0.5254	5.4800e-011	0.3119	0.3446
10_g	0.4515	0.4240	0.4935	5.1685e-011	0.3048	0.3002
11_g	0.5895	0.6696	0.7858	2.9179e-007	3.7750	4.1048e+004
12_g	0.4796	0.4622	0.5407	7.1540e-011	0.3472	0.5457
13_g	0.3978	0.4367	0.5249	5.7391e-011	0.3062	0.3196
14_g	0.4131	0.4226	0.4814	4.8108e-011	0.2704	0.1902
15_g	0.4283	0.4066	0.4674	4.5561e-011	0.2937	0.2401

help the execution. The proposed segmentation strategies have been assessed in a database of 650 images with OD and OC limits physically set apart via trained experts. The segmented OD and OC are then used to process the CDR for glaucoma screening. The technique accomplishes AUC of 0.800 and 0.822 in two different databases, which is higher than other strategies. The techniques can be utilized for glaucoma screening. The effective quantitative imaging alternatives for the detection and management of glaucoma. Several imaging modalities and their enhancements, including optical coherence tomography and multifocal electro retinograph are prominent techniques employed to quantitatively analyze structural and functional abnormalities in the eye both to observe variability and to quantify the progression of the disease objectively. Automated clinical decision support systems (CDSSs) in ophthalmology, such as CASNET/glaucoma are designed to create effective decision support systems for the identification of disease pathology in human eyes.

Table 5. Healthy image diagonal detail

Image	Red	Average Green	Blue	Energy	Standard Deviation	Variance
1_h	0.2285	0.2344	0.2560	3.8383e-012	0.0454	2.6882e-004
2_h	0.2542	0.2429	0.2617	4.4430e-012	0.0492	3.6265e-004
3_h	0.2590	0.2477	0.2705	4.8065e-012	0.0537	4.7968e-004
4_h	0.2390	0.2293	0.2467	3.5597e-012	0.0423	2.3726e-004
5_h	0.2358	0.2330	0.2541	3.7117e-012	0.0438	2.5080e-004
6_h	0.2342	0.2223	0.2418	3.2085e-012	0.0399	1.6688e-004
7_h	0.2042	0.2312	0.2532	3.8611e-012	0.0493	4.2539e-004
8_h	0.2263	0.2294	0.2469	3.5275e-012	0.0413	2.1406e-004
9_h	0.2024	0.1940	0.2086	2.0859e-012	0.0323	7.7290e-005
10_h	0.1139	0.2137	0.2316	2.8535e-012	0.0367	1.6540e-004
11_h	0.1734	0.2032	0.2184	2.4664e-012	0.0335	9.8718e-005
12_h	0.1999	0.2044	0.2209	2.6008e-012	0.0349	1.1299e-004
13_h	0.1889	0.1944	0.2124	2.0995e-012	0.0311	7.7913e-005
14_h	0.2123	0.2018	0.2144	2.3296e-012	0.0288	5.6364e-005
15_h	0.1932	0.2201	0.2435	3.1807e-012	0.0381	1.7156e-004

Table 6. Glaucoma image diagonal detail

| Image	Red	Average Green	Blue	Energy	Standard Deviation	Variance
1_g	0.1548	0.2353	0.2536	4.7799e-012	0.0670	0.0011
2_g	0.1877	0.2347	0.2488	3.9901e-012	0.0485	3.0642e-004
3_g	0.1321	0.2236	0.2414	3.1381e-012	0.0389	1.5426e-004
4_g	0.1723	0.2372	0.2569	4.0093e-012	0.0432	2.3126e-004
5_g	0.1849	0.2214	0.2420	3.2582e-012	0.0434	2.5581e-004
6_g	0.2081	0.1983	0.2139	2.2808e-012	0.0355	1.4045e-004
7_g	0.1090	0.2261	0.2455	3.5995e-012	0.0452	3.2754e-004
8_g	0.1439	0.2070	0.2237	2.6756e-012	0.0373	1.7287e-004
9_g	0.1720	0.2211	0.2431	3.2330e-012	0.0400	1.8912e-004
10_g	0.2146	0.2113	0.2245	2.7072e-012	0.0368	1.3646e-004
11_g	0.2162	0.2089	0.2302	2.7315e-012	0.0346	1.0772e-004
12_g	0.2182	0.2205	0.2363	3.2593e-012	0.0406	2.0156e-004
13_g	0.1717	0.1995	0.2170	2.4236e-012	0.0310	7.1496e-005
14_g	0.1770	0.1855	0.1991	1.9719e-012	0.0348	6.5016e-005
15_g	0.1998	0.1994	0.2112	2.3862e-012	0.0392	1.3793e-004
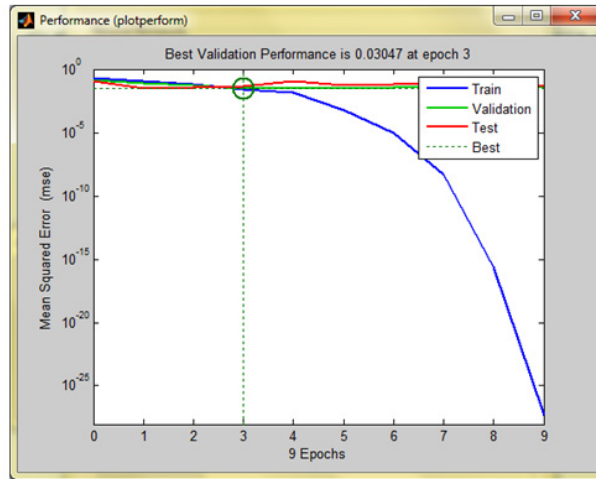
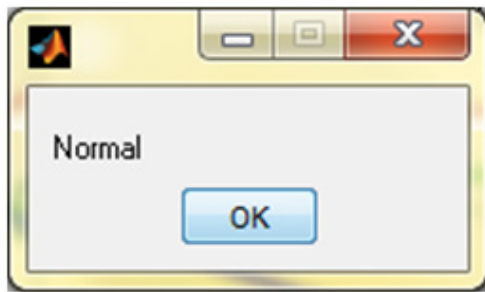**Fig. 6.** GUI showing performance validation using NN classifier for normal image

Fig.7. GUI showing classifier output – Normal

Texture assumes a critical part in numerous machine vision errands, for example, surface examination, scene classiûcation, surface introduction and shape assurance. Texture is portrayed by the spatial dissemination of gray levels in an area. Analysis of texture requires the identiûcation of proper attributes or features that differentiate the textures in the image for segmentation, classiûcation and recognition. The features are assumed to be uniform within the regions containing the same textures. Textural
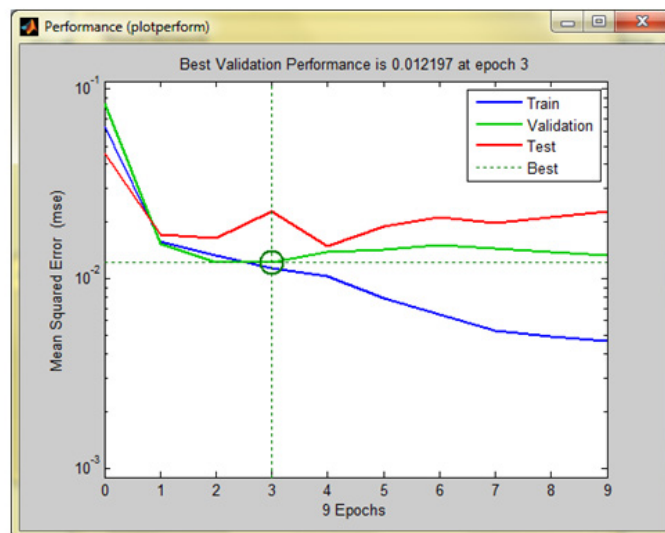

Fig.8. GUI showing performance validation using NN classifier for abnormal image

features are, consequently, not bound to particular areas on the image. A few component extraction systems, including spectral procedures, are accessible to mine texture features. The utilization of texture features and HOS were proposed for glaucomatous classification. In spite of the fact that the texture based strategies have been demonstrated effective, it is as yet a test to produce includes that recover summed up auxiliary and textural features from retinal images. Textural features utilizing Wavelet Transforms (WTs) in image processing are frequently utilized to conquer the generalization of features.

Datasets

   This database was recognized by a study group to carry proportional studies on automatic segmentation algorithms on fundus images. The public dataset examples shown in Figure.2 consist of 15 healthy fundus, 15 DR images and 15 glaucomatous images. Binary gold standard vessel segmentation images are available and also masks influential FOV are provided.

Proposed system

   The objective of this work is to differentiate normal eye images and glaucoma affected eye images. This classification is based on selecting eminent features using wavelet filters. The wavelet features are used to train the supervised classifier which classifies retinal images into normal or abnormal and achieve a high a level of accuracy as

shown in Figure.3. It is proposed to use a wavelet filter is daubechies. This filter is used to calculate energy and average value for the image. With the help of this filter, the wavelet coefficients are obtained and their characteristics like average, energy, standard deviation and variance are resulting in feature extraction. This filter will increase the accuracy and performance of an image. This filter is examined by employing a standard 2-D discrete wavelet transform (DWT) which are used to extract features and analyze changes. The extracted features are fed into supervised classifier such as Neural Network.

   The figure 6.1 describes about the overall process architecture of our project. There will be sets like training set and testing set. In training set the input images that are to be trained are preprocessed. The preprocessing is carried out like scaling and selecting green channel. Then from the preprocessed input images, features like average, energy, standard deviation and variance are extracted. Then these extracted features are fed into Neural Network classifier for classification process. In testing set, each image that is tested whether it is normal or abnormal

Preprocessing

   The objective of preprocessing is to improve the interoperability of the information present in images for human viewers. An enhancement algorithm is one that yields a

Table 7. Performance measurement

Classes	No. of Training Images	No. of Testing Images	No. of Correctly Classified Images	Classification Accuracy (%)
Normal	05	12	12	100
Glaucoma	05	12	11	91.67
Average Accuracy	95.83			

Table 8. Performance comparison of Glaucoma classification

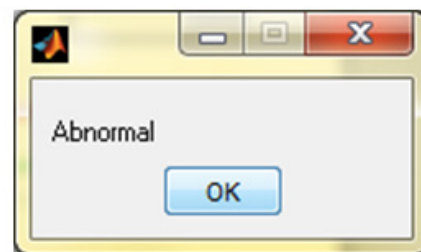| Methodologies	Year	Accuracy (%)
Proposed work	2017	95.83
Kiran SM et al [13]	2016	91.66
N.Annu et al [14]	2013	95.00

Fig. 9. GUI showing classifier output – Abormal

better quality image for the purpose of some particular application which can be done by either suppressing the noise or increasing the image contrast. Image preprocessing includes emphasis, sharpen or smoothen image features for display and analysis. Enhancement methods are application specific and are often developed empirically. Image preprocessing techniques emphasis specific image features to improve the visual perception of an image.

Image decompositon using wavelet transforms

The DWT confine the spatial and frequency information's of an indication. DWT breaks down the image by disintegrating it into a coarse estimate through low-pass filtering and into detail data by means of high-pass filtering. Such decay is performed recursively on low-pass estimate coefficients got at each level, until the point when the vital emphases are come to. Each image is represented to as a p × q gray scale network I [i,j], where every component of the framework speaks to the grayscale intensity of one pixel of the image. Each nonborder pixel has eight nearby neighboring pixel intensities. These eight neighbors can be utilized to navigate the network. The resultant 2-D DWT coefficients are the same regardless of whether the lattice is crossed ideal left-to-right or right-to-left. Henceforth, it is adequate that we consider four directions comparing to 0æ% (Dh), 45æ% (Dd), 90æ% (Dv), and 135æ% (Dd) orientations. The decay structure for one level is represented in Figure.4. In this work daubechies (db4) wavelet filter is used. After decomposition, it reproduces the original image without loss of any information. The proposed system contains features of average or mean, energy, standard deviation and variance.

Feature extraction

It is used to select important features of an image. Feature extraction is a particular form of dimensionality reduction. If the input data is too large to be processed, then the input information will be transformed into a condensed set of features (also named features vector). The features extracted are carefully chosen such a way that they will extract the relevant information to carry out the desired task. This approach is successful when images are large and an optimized features is required to complete tasks quickly.

Investigation with an extensive number of factors by and large requires a lot of memory and computation control or classification method which over fits the training sample and sums up inadequately to new examples. Best outcomes are accomplished when a specialist develops an arrangement of use of application dependent features.

Average or mean

Average feature helps to measure the center tendency of data. Average is Add up all the numbers (pixels) and then divided by the number of pixels. It is calculated from the decomposition image in directions of horizontal, vertical and diagonal as stated in Equation (1 to 3).

$$\text{Average Dh1} = \frac{1}{p \times q} \sum_{x=\{p\}} \sum_{y=\{q\}} |Dh1(x,y)|$$
...(1)

$$\text{Average Dv1} = \frac{1}{p \times q} \sum_{x=\{p\}} \sum_{y=\{q\}} |Dv1(x,y)|$$
...(2)

$$\text{Average Dd1} = \frac{1}{p \times q} \sum_{x=\{p\}} \sum_{y=\{q\}} |Dd1(x,y)|$$
...(3)

Energy

It is the proportion of each channel takes up in original color image or which channel (Red, Green and Blue) has the bigger proportion and has been calculated as stated in Equation (4 to 6)

$$\text{Energy} = \frac{1}{p^2 \times q^2} \sum_{x=\{p\}} \sum_{y=\{q\}} \left(Dh1(x,y)\right)^2$$
...(4)

$$\text{Energy} = \frac{1}{p^2 \times q^2} \sum_{x=\{p\}} \sum_{y=\{q\}} \left(Dv1(x,y)\right)^2$$
...(5)

$$\text{Energy} = \frac{1}{p^2 \times q^2} \sum_{x=\{p\}} \sum_{y=\{q\}} \left(Dd1(x,y)\right)^2$$
...(6)

Standard deviation

The standard deviation (SD) as stated in Equation (7) describes the variation from the

average exists. A low SD point towards that the data points are close to the mean. A high SD point towards that the data points are extensive over huge values.

$$s_x = \sqrt{\frac{\sum_{i=1}^{n}(x_i - \bar{x})^2}{n - 1}}$$

n = The number of data points

$\bar{x}$ = The mean of the x_i

x_i = Each of the values of the data

...(7)

Variance

The difference measures how far an arrangement of numbers is spread out. (A difference of zero demonstrates that every one of the qualities are indistinguishable.) Variance is dependably non-negative. A little fluctuation demonstrates that the information directs incline toward be near the mean (expected esteem) and henceforth to each other, while a high change shows that the information calls attention to extremely spread out from the mean and from each other. The square foundation of change is known as the standard deviation. Square of standard deviation gives an estimate spread of pixel value around the image mean.

Image classification

Classification of data is used to assign corresponding levels with the aim of discriminating multiple objects from each other within the image. The level is called as class. Classification will be executed on the base of spectral or spectrally defined features, such as density, texture etc. It can be said that classification divides the feature space into several classes based on a decision rule. In this work, the classification process has been carried out as per the flow diagram shown in Figure. 5.

Neural systems are made out of basic components working in parallel. These components are motivated by natural sensory systems. As in nature, the associations between components generally decide the system work. Neural system can be prepared to play out a specific capacity by changing the estimations of the associations (weights) between components. Commonly, neural systems are balanced, or prepared, with the goal that a specific info prompts a particular target yield. The system is balanced, in light of a correlation of the yield and the objective, until the point when the system yield coordinates the objective. Regularly, numerous such info/target sets are expected to train the system.

RESULTS AND DISCUSSION

The feature information extracted for healthy and glaucomatous input image along horizontal, vertical and diagonal axis is tabulated in Table 1 to Table 6. The values are calculated for average for red, green and blue channels. Energy, standard deviation and variance are calculated for green channel.

The features along horizontal, vertical and diagonal axis of the image extracted are fetched as input to FFBNN classifier in order to train and test the system. The neural network performance platform and the classification output for both healthy and abnormal image is shown in Figure.6 to Figure.9.

Table 7 gives the results of the proposed work on HRF dataset shows the performance evaluation of classification of fundus image, and an average sensitivity rate of 100% and specificity rate of 91.67% and accuracy rate of 95.83% on HRF dataset are obtained.

Table 8 shows the performance comparisons of the proposed classification methodology with the authors Kiran S.M *et al* (2016) and N.Annu *et al* (2013). The proposed methodology achieves 95.83% average accuracy compared with the Kiran S.M *et al* (2016) achieves 91.66% of an average accuracy and N.Annu *et al* (2013) achieves 95% of an average accuracy. This proposed classification methodology on HRF dataset provides better sensitivity and higher accuracy.

CONCLUSION

The proposed method to classify the fundus image into normal and glaucomatous image is carried out in this work. The results obtained yield an accuracy rate of 95.83%. The study also illustrates the efficacy of wavelet-based feature techniques for detecting and predicting glaucomatous progression. From the accuracies obtained, it can be concluded that the average, energy, standard deviation and variance are obtained from the detailed coefficients that can be used to distinguish between normal

and glaucomatous images with very high level accuracy.

REFERENCES

1. Sisodia D.S, Nair S, Khobragade P, "Diabetic Retinal Fundus Images: Preprocessing and Feature Extraction for Early Detection of Diabetic Retinopathy" *Biomed Pharmacol J,* **10**(2): pp.no.615-626 (2017)

2. Kiran SM and Chandrappa DN, "Automatic Detection of Glaucoma using 2-D DWT", *International Research Journal of Engineering and Technology,* **3**(6), pp.no.201-205 (2016).

3. Ganesh Babu, TR, Sathishkumar, R & Rengarajvenkatesh, "Segmentation of optic nerve head for glaucoma detection using fundus images", *Biomedical and Pharmacology Journal,* **7**(2), pp.no.697-705 (2014).

4. Annu N and Judith Justin, "Automated Classification of Glaucoma Images by Wavelet Energy Features", *International Journal of Engineering and Technology,* **5**(2), pp.no.1716-1721 (2013).

5. Paul Y. Kim, Khan M. Iftekharuddin, Pinakin G. Davey, Márta Tóth, Anita Garas, Gabor Holló, Edward A. Essock, "Novel Fractal Feature-Based Multiclass Glaucoma Detection and Progression Prediction" *IEEE Journal of Biomedical and Health Informatics,* **17**(2), pp.no.269 – 276 (2013).

6. Jun Cheng, Jiang Liu, Yanwu Xu, Fengshou Yin, Damon Wing Kee Wong, Ngan-Meng Tan, Dacheng Tao, Ching-Yu Cheng, Tin Aung, Tien Yin Wong, "Superpixel Classification Based Optic Disc and Optic Cup Segmentation for Glaucoma Screening" *IEEE Transactions on Medical Imaging,* **32**(6): pp.no.1019 – 1032 (2013).

7. Dua, Sumeet, U. Rajendra Acharya, Pradeep Chowriappa, and S. Vinitha Sree. "Wavelet-Based Energy Features for Glaucomatous Image Classification", IEEE Transactions on Information Technology in Biomedicine, (2012).

8. U. Rajendra Acharya, Sumeet Dua, Xian Du, Vinitha Sree S, Chua Kuang Chua, "Automated Diagnosis of Glaucoma Using Texture and Higher Order Spectra Features" *IEEE Transactions on Information Technology in Biomedicine,* **15**(3): pp.no.449–455 (2011).

9. M.Balasubramanian *et al.*, "Clinical evaluation of the proper orthogonal decomposition framework for detecting glaucomatous changes in human subjects, *Invest Ophthalmol Vis Sci.,* **51**(1), pp.no.264–271 (2010).

10. J.M. Miquel-Jimenez *et al.*, "Glaucoma detection by wavelet-based analysis of the global flash multifocal electroretinogram" *Med. Eng. Phys.,* **32** pp. 617–622 (2010).

11. Ke Huang, Selin Aviyente, 'Wavelet Feature Selection for Image Classification' *IEEE Transactions on Image Processing,* **17**(9), pp.no.1709 - 1720 (2008).

12. S.Arivazhagan, L.Ganesan, 'Texture segmentation using wavelet transform' *Pattern Recognition Letters,* **24**, pp.no.3197–3203 (2003).